

# Blind Estimation of Symbol Timing and Carrier Frequency Offset in Wireless OFDM Systems

Helmut Bölcskei, *Member, IEEE*

**Abstract**—Orthogonal frequency-division multiplexing (OFDM) systems are highly sensitive to synchronization errors. In this paper, we introduce an algorithm for the blind estimation of symbol timing and carrier frequency offset in wireless OFDM systems. The proposed estimator is an extension of the Gini-Giannakis estimator for single-carrier systems. It exploits the cyclostationarity of OFDM signals and relies on second-order statistics only. Our method can be applied to pulse shaping OFDM systems with arbitrary time-frequency guard regions, OFDM based on offset quadrature amplitude modulation, and biorthogonal frequency-division multiplexing systems. We furthermore propose the use of different subcarrier transmit powers (subcarrier weighting) and periodic transmitter precoding to achieve a carrier frequency acquisition range of the entire bandwidth of the OFDM signal, and a symbol timing acquisition range of arbitrary length. Finally, we provide simulation results demonstrating the performance of the new estimator.

**Index Terms**—Blind estimation, cyclostationarity, orthogonal frequency-division multiplexing (OFDM), pulse shaping, synchronization.

## I. INTRODUCTION AND OUTLINE

RECENTLY, orthogonal frequency-division multiplexing (OFDM) [2]–[5] has received considerable attention. It has been adopted or proposed for a number of applications, such as satellite and terrestrial digital audio broadcasting (DAB), digital terrestrial TV broadcasting (DVB), broadband indoor wireless systems, asymmetric digital subscriber line (ADSL) for high bit-rate digital subscriber services on twisted-pair channels, and fixed broadband wireless access. Important features of OFDM systems include immunity to multipath fading and impulsive noise [6]. Since the individual subcarrier signal spectra are affected by frequency-flat rather than frequency-selective fading, equalization is drastically simplified [2].

Unfortunately, OFDM systems are far more sensitive to synchronization errors than single-carrier systems [7]. Most OFDM time-frequency offset estimators proposed in the literature require pilot symbols or training sequences (e.g., [8]–[11]). How-

ever, the use of training data lowers the achievable data rate. Therefore, alternative methods that do not make use of pilot symbols or training sequences are desirable. Such estimators [12], [13] typically exploit the redundancy introduced by the cyclic prefix (CP).

In this paper, we present a novel algorithm for the blind estimation<sup>1</sup> of symbol timing and carrier frequency offset in pulse shaping OFDM systems. Our method can be used for broadcasting applications and in the downlink of OFDM-based mobile radio systems. The proposed estimator is an extension of the Gini-Giannakis estimator [1] for single-carrier systems. It relies on second-order statistics only and exploits the cyclostationarity [14] of the OFDM signal. Furthermore, we propose the use of different subcarrier transmit powers (subcarrier weighting) and a form of periodic transmitter precoding to drastically increase the estimator's acquisition range. We shall next summarize important features of the novel method as follows.

- It applies to *pulse shaping OFDM* and biorthogonal frequency-division multiplexing (BFDM) [15], [16] systems with *arbitrary pulse shapes* and *arbitrary time-frequency guard regions* [6], [5], [15], and to OFDM based on offset QAM (OFDM/OQAM) [17], [16].
- It is capable of performing a *carrier frequency acquisition over the entire bandwidth of the OFDM signal*.
- It applies to *noninteger timing errors*.
- A form of periodic transmitter precoding yields a *symbol timing acquisition range of arbitrary length*.
- It applies to *time-dispersive environments* provided the channel can be estimated separately.
- *It does not necessarily need a CP* (in this case, the estimators proposed in [12] and [13] would break down).
- It is fast Fourier transform (FFT)-based and hence *computationally efficient*.
- The estimators are *asymptotically unbiased and consistent*.
- It *exhibits small sensitivity to stationary noise*.

The paper is organized as follows. In Section II, we briefly review the different types of pulse shaping OFDM systems considered in the paper, and we provide our assumptions and the problem statement. Section III discusses possibilities of evoking cyclostationarity in OFDM signals. Section IV introduces the new estimators and discusses their properties. Section V presents simulation results, and Section VI concludes the paper.

<sup>1</sup>The estimation is blind because it does not need pilot symbols or training sequences. In fact, it does not even need a CP.

Paper approved by B. L. Hughes, the Editor for Theory and Systems of the IEEE Communications Society. Manuscript received October 7, 1999; revised November 21, 2000. This paper was presented in part at IEEE ICASSP'99, Phoenix, AZ, March 1999.

The author was with the Information Systems Laboratory, Stanford University, Stanford, CA 94305-9510 USA, on leave from the Institut für Nachrichtentechnik und Hochfrequenztechnik, Technische Universität Wien, Vienna, Austria. He is now with the Coordinated Science Laboratory and Department of Electrical Engineering, University of Illinois, Urbana IL 61801 USA (e-mail: bolcskei@uiuc.edu).

Publisher Item Identifier S 0090-6778(01)04867-X.

## II. PULSE SHAPING OFDM AND BFDM SYSTEMS

In this section, we shall briefly review the different types of pulse shaping OFDM systems considered in the paper, namely OFDM and BFDM employing time-frequency guard regions [6], [5], [15], and OFDM and BFDM based on offset QAM (OFDM/OQAM and BFDM/OQAM, respectively) [17], [16]. In the following, both OFDM and BFDM schemes will be simply referred to as OFDM.

### A. OFDM Employing Time-Frequency Guard Regions

The baseband equivalent of a pulse shaping OFDM signal is given by

$$x[n] = \sum_{k=0}^{N-1} \sum_{l=-\infty}^{\infty} c_{k,l} g[n-lM] e^{j(2\pi/N)k(n-lM)} \quad (1)$$

where  $N$  is the number of subcarriers,  $M$  is the symbol length,  $g[n]$  denotes the transmitter pulse shaping filter, and  $c_{k,l}$  denotes the data symbols (taken from a finite complex alphabet constellation). For  $M > N$ , the system is said to employ a time-frequency guard region [6], [5], [18], [15]. In fact, CP OFDM [2] can be seen as a special case thereof with the time-frequency guard region being a temporal guard region only. Note, however, that  $M > N$  can be achieved not only by insertion of a CP; for example, one can introduce *spectral guard regions* by spacing the subcarriers further apart to reduce (or avoid) intercarrier interference (ICI) caused by frequency-dispersion. In time-frequency dispersive environments (such as mobile radio channels), in general, it will be desirable to have both temporal and spectral guard regions.

In the following,  $h[n]$  denotes the receiver pulse shaping filter and  $\langle a, b \rangle = \sum_{n=-\infty}^{\infty} a[n]b^*[n]$  is the inner product of the sequences  $a[n]$  and  $b[n]$ . In the OFDM case,  $h[n] = g[n]$  is orthogonal in the sense that  $\langle g, g_{k,l} \rangle = \delta[k]\delta[l]$ , whereas in the BFDM case,  $g[n]$  and  $h[n]$  constitute a biorthogonal pair [15], [16], i.e.,  $\langle g, h_{k,l} \rangle = \delta[k]\delta[l]$ . The real-valued pulses  $g[n]$  and  $h[n]$  are biorthogonal if their cross-ambiguity function [19]  $A^{(g,h)}[k, \theta] = \sum_{n=-\infty}^{\infty} g[n]h[n-k]e^{-j2\pi n\theta}$  satisfies

$$A^{(g,h)}\left[lM, \frac{k}{N}\right] = \delta[l]\delta[k], \quad l \in \mathbb{Z}, k \in [0, N-1]. \quad (2)$$

For  $h[n] = g[n]$ , (2) reduces to  $A^{(g,g)}[lM, (k/N)] = \delta[l]\delta[k]$ .

The use of time-frequency well-localized pulse shaping filters is of particular importance in time-frequency dispersive environments (such as the mobile radio channel), since here good time-frequency localization of the transmitter basis functions avoids the symbol energy “spreading out” and perturbing neighboring symbols in the time-frequency plane [5], [18]. Further advantages of pulse shaping are reduced out-of-band emission in wireless OFDM, reduced sensitivity to carrier frequency offsets, and the possibility to perform blind synchronization (to be shown in the paper). In an OFDM system employing a CP [2]  $g[n]$  is a rectangular pulse of length  $M = N + L$ , where  $L$  denotes the length of the CP and  $h[n]$  is a rectangular pulse of duration  $N$ .

### B. OFDM/OQAM

It has been pointed out in [5], [6], and [16] that in contrast to QAM-based OFDM systems<sup>2</sup> (discussed in Section II-A) OFDM/OQAM allows time-frequency well-localized transmitter basis functions even for critical lattice density  $M = N$ , i.e., maximum spectral efficiency. In fact, in [16] it is shown that an OFDM/OQAM system with  $M = N$  achieves the same pulse shaping filter quality (in terms of time-frequency localization) as an OFDM/QAM system with  $M = 2N$ . For high-data-rate applications, OFDM/OQAM therefore seems to be an interesting alternative to OFDM/QAM.

In an  $N$ -channel OFDM/OQAM system (assuming that  $N = M$  is even) we have

$$x[n] = \sum_{k=0}^{M-1} \left[ \sum_{l=-\infty}^{\infty} c_{k,l}^R g[n-lM] e^{j(2\pi/M)k(n-\alpha/2)} + \sum_{l=-\infty}^{\infty} j c_{k,l}^I g[n+M/2-lM] e^{j(2\pi/M)k(n-\alpha/2)} \right] \quad (3)$$

where  $c_{k,l}^R = \text{Re}\{c_{k,l}\}$  and  $c_{k,l}^I = \text{Im}\{c_{k,l}\}$  denote the real and imaginary parts of the data symbols  $c_{k,l}$ , respectively, and  $\alpha \in [0, M-1]$ . For  $g[n]$  supported in  $[0, L_g-1]$ , the constant  $\alpha$  has to be chosen as  $\alpha = (L_g + (M/2) - 1) \bmod M$  [16]. The real-valued pulse  $g[n]$  is orthogonal if

$$A^{(g,g)}\left[lM, 2\frac{k}{M}\right] = \delta[l]\delta[k], \quad l \in \mathbb{Z}, k \in [0, M/2-1]. \quad (4)$$

For more details on OFDM/OQAM and BFDM/OQAM, the interested reader is referred to [16].

### C. Assumptions and Problem Statement

**Assumptions:** The timing uncertainty in the OFDM signal will be modeled as a time shift, and the unknown carrier frequency offset is accounted for by a frequency shift. The received OFDM signal is therefore given by

$$r[n] = e^{j(2\pi\theta_e n + \phi)} \int_0^1 X(e^{j2\pi\nu}) e^{j2\pi\nu(n-n_e)} d\nu + \rho[n] \quad (5)$$

where  $n_e \in \mathbb{R}$  is the timing offset,  $\theta_e \in [-1/2, 1/2)$  denotes the carrier frequency offset,  $\phi$  is the initial phase, and  $\rho[n]$  is a wide-sense stationary noise process, independent of the data symbols  $c_{k,l}$ . Note that the timing offset  $n_e$  is not restricted to be an integer multiple of the chip period. For  $n_e \in \mathbb{Z}$ , (5) simplifies to

$$r[n] = e^{j(2\pi\theta_e n + \phi)} x[n - n_e] + \rho[n]. \quad (6)$$

The correlation function of the noise process is given by<sup>3</sup>  $c_\rho[\tau] = \mathcal{E}\{\rho[n]\rho^*[n-\tau]\}$ . The symbols  $c_{k,l}$  drawn from a

<sup>2</sup>Note that the symbol constellation in the OFDM systems discussed in Section II-A is not really limited to QAM. In fact, the  $c_{k,l}$  can be taken from an arbitrary constellation. We chose the terminology of OFDM/QAM to emphasize the difference between the OFDM systems discussed in Section II-A and OFDM based on OQAM discussed in this subsection.

<sup>3</sup> $\mathcal{E}$  denotes the expectation operator.

finite-alphabet complex constellation satisfy  $\mathcal{E}\{c_{k,l}c_{k',l'}^*\} = \sigma_c^2 \delta[k - k'] \delta[l - l']$ . We furthermore assume that  $\mathcal{E}\{c_{k,l}^R c_{k',l'}^R\} = \sigma_{c,R}^2 \delta[k - k'] \delta[l - l']$ ,  $\mathcal{E}\{c_{k,l}^I c_{k',l'}^I\} = \sigma_{c,I}^2 \delta[k - k'] \delta[l - l']$ , and  $\mathcal{E}\{c_{k,l}^R c_{k',l'}^I\} = 0$ . The initial discussion is restricted to the additive white Gaussian noise (AWGN) case. The time-dispersive case will be treated in the last paragraph of Section IV-A.

**Subcarrier Weighting:** We furthermore assume that the individual subcarriers are transmitted with different powers, or equivalently, we perform subcarrier weighting. The weighting function is given by  $w[k] \in \mathbb{C}$ , i.e., the symbols on the  $k$ th subcarrier are multiplied by  $w[k]$ . In the OFDM/QAM case, the transmit signal is therefore given by

$$x[n] = \sum_{k=0}^{N-1} \sum_{l=-\infty}^{\infty} c_{k,l} w[k] g[n - lM] e^{j(2\pi/N)k(n-lM)}. \quad (7)$$

The OFDM/OQAM transmit signal reads

$$\begin{aligned} x[n] = & \sum_{k=0}^{M-1} w[k] \\ & \cdot \left[ \sum_{l=-\infty}^{\infty} c_{k,l}^R g[n - lM] e^{j(2\pi/M)k(n-\alpha/2)} \right. \\ & \left. + \sum_{l=-\infty}^{\infty} j c_{k,l}^I g[n + M/2 - lM] e^{j(2\pi/M)k(n-\alpha/2)} \right]. \end{aligned} \quad (8)$$

Consequently, in the receiver the symbols corresponding to the  $k$ th subchannel have to be divided by  $w[k]$ . Subcarrier weighting will be seen later to drastically increase the carrier frequency acquisition range. We finally note that in the OFDM system proposed for DVB, it is suggested to increase the transmit power of every 12th subcarrier by 77% to facilitate (nonblind) synchronization. This can be seen as a special case of subcarrier weighting.

**Problem Statement:** We want to derive estimates of the timing error  $n_e$  and the carrier frequency offset  $\theta_e$  from consecutive samples of the received signal  $r[n]$ . If the data symbols  $c_{k,l}$  are known, which corresponds to a data-aided (nonblind) scenario, and the distribution of  $\rho[n]$  is known, then maximum-likelihood (ML) estimation of  $n_e$  and  $\theta_e$  is possible although computationally demanding. For unknown data, an ML approach for estimating  $n_e$  and  $\theta_e$  in CP OFDM systems has been proposed in [13]. This approach, however, requires knowledge of the distributions of  $x[n]$  and  $\rho[n]$ , and cannot directly be applied to pulse shaping OFDM systems. In this paper, we aim at consistent, computationally efficient estimates that do not require knowledge of the distributions of  $x[n]$  and  $\rho[n]$ , and apply to the blind (nondata-aided) case with arbitrary stationary noise processes  $\rho[n]$ . Throughout the paper, we assume that the receiver knows the pulse shaping filter  $g[n]$ , the subcarrier weights  $w[k]$ , and the variances  $\sigma_c^2$ ,  $\sigma_{c,R}^2$ , and  $\sigma_{c,I}^2$ .

### III. CYCLOSTATIONARITY IN OFDM SYSTEMS

As already mentioned in Section I, cyclostationarity is the key to blind synchronization. In this section, we shall discuss various

ways of evoking cyclostationarity in OFDM signals. The following results constitute the basis for the estimators presented in Section IV.

#### A. Cyclostationarity in OFDM/QAM Systems

Let us first consider pulse shaping OFDM/QAM systems employing time-frequency guard regions and subcarrier weighting. With the transmit signal given by (7), we shall next show that under quite general conditions the received signal  $r[n]$  in (5) is cyclostationary (CS) [14]. The correlation function of a (nonstationary) stochastic process is defined as  $c_r[n, \tau] = \mathcal{E}\{r[n]r^*[n - \tau]\}$ , where  $\tau$  is an integer lag parameter.<sup>4</sup> The signal  $r[n]$  is said to be second-order CS with period  $M$  if  $c_r[n, \tau] = c_r[n + M, \tau]$  [14]. It is shown in the Appendix that the correlation function of the received OFDM signal  $r[n]$  is given by

$$\begin{aligned} c_r[n, \tau] = & \frac{\sigma_c^2}{M} e^{j2\pi\theta_e\tau} \Gamma_N[\tau] \sum_{u=-\infty}^{\infty} g[u]g[u - \tau] \\ & \cdot \sum_{s=0}^{M-1} e^{-j2\pi(s/M)(u-n+n_e)} + c_\rho[\tau], \quad n_e \in \mathbb{R} \end{aligned} \quad (9)$$

which simplifies to

$$\begin{aligned} c_r[n, \tau] = & \sigma_c^2 e^{j2\pi\theta_e\tau} \Gamma_N[\tau] \sum_{l=-\infty}^{\infty} g[n - n_e - lM] \\ & \cdot g[n - n_e - lM - \tau] + c_\rho[\tau] \end{aligned} \quad (10)$$

for  $n_e \in \mathbb{Z}$ . Here,  $\Gamma_N[\tau] = \sum_{k=0}^{N-1} |w[k]|^2 e^{j(2\pi/N)k\tau}$  is the  $N$ -point inverse discrete Fourier transform (DFT) of  $|w[k]|^2$ . From (9), it follows that  $c_r[n, \tau]$  is  $M$ -periodic in  $n$  for every  $\tau$ , i.e.,  $c_r[n, \tau] = c_r[n + M, \tau]$ . Note that for  $|w[k]| = 1$  ( $k = 0, 1, \dots, N-1$ ) (i.e., equal transmit power on all subcarriers), we have  $\Gamma_N[\tau] = N \sum_{s=-\infty}^{\infty} \delta[\tau - sN]$ , which implies that  $c_r[n, \tau] = c_\rho[\tau]$  for  $\tau \neq sN$  with  $s \in \mathbb{Z}$ .

There are different possibilities of introducing cyclostationarity in OFDM signals, either by the use of time-frequency guard regions (like a CP, for example), by employing pulse shaping, by the use of different transmit powers on the subcarriers [20], and finally by periodic transmitter precoding as discussed in Section IV-B. In the following, we shall discuss these methods in detail.

**No Pulse Shaping and No Guard Regions:** Consider the case of no time-frequency guard regions (i.e.,  $M = N$ ) and no pulse shaping, i.e.,  $h[n] = g[n] = (1/\sqrt{M})$  for  $n \in [0, M-1]$  and 0 else. (We note that these specifications will hardly be used in practical OFDM systems.) If no subcarrier weighting is employed (i.e.,  $|w[k]| = 1$  for  $k \in [0, M-1]$ ), it is easily verified that  $c_r[n, \tau] = (\sigma_c^2/M)\delta[\tau] + c_\rho[\tau]$  for  $n_e \in \mathbb{R}$ , and hence no information on the synchronization parameters  $n_e$  and  $\theta_e$  is contained in  $c_r[n, \tau]$ . We shall next demonstrate that if subcarrier weighting is employed the signal  $r[n]$  becomes CS and information on the timing error and the carrier frequency offset can

<sup>4</sup>For stationary processes, the correlation function  $c_r[n, \tau]$  is a function of the lag parameter  $\tau$  only.

be extracted from the second-order statistics of  $r[n]$ . For general  $w[k]$  and  $n_e \in \mathbb{Z}$ , we obtain

$$c_r[n, \tau] = \sigma_c^2 e^{j2\pi\theta_e\tau} \Gamma_M[\tau] a_M^{(\tau)}[n - n_e] + c_\rho[\tau] \quad (11)$$

where  $a_M^{(\tau)}[n] = \sum_{l=-\infty}^{\infty} a^{(\tau)}[n - lM]$  is an  $M$ -periodized version of  $a^{(\tau)}[n] = g[n]g[n-\tau]$ . Note that  $c_r[n, \tau] = c_\rho[\tau]$  for  $|\tau| \geq M$ . Similar expressions can be given for  $n_e \in \mathbb{R}$ . Now, if the subcarrier weights  $w[k]$  are chosen such that  $\Gamma_M[\tau] \neq 0$  for at least one<sup>5</sup>  $\tau \in [1, M-1]$ , the correlation function  $c_r[n, \tau]$  contains information on both synchronization parameters.

**Biorthogonal Case Without Guard Regions:** Still assuming that no time-frequency guard regions are employed (i.e.,  $N = M$ ) and using pulse shaping (with nonoverlapping pulse shaping filters),<sup>6</sup> we shall next show that the signal  $r[n]$  is CS. Take  $g[n] \neq 0$  for  $n \in [0, M-1]$  and 0 else. It can be verified that  $h[n] = (1/Mg[n])$  for  $n \in [0, M-1]$  and 0 else satisfies the biorthogonality condition (2). If no subcarrier weighting is employed (i.e.,  $|w[k]| = 1$ ), we get  $c_r[n, \tau] = \sigma_c^2 \delta[\tau] \sum_{u=0}^{M-1} g^2[u] \sum_{s=0}^{M-1} e^{-j2\pi(s/M)(u-n+n_e)} + c_\rho[\tau]$  for  $n_e \in \mathbb{R}$ , and  $c_r[n, \tau] = \sigma_c^2 M \delta[\tau] a_M^{(0)}[n - n_e] + c_\rho[\tau]$  for  $n_e \in \mathbb{Z}$ , where  $a_M^{(0)}[n] = \sum_{l=-\infty}^{\infty} g^2[n - lM]$  is an  $M$ -periodized version of  $g^2[n]$ . The second-order statistics of  $r[n]$  contain timing information only. We shall next demonstrate that the use of subcarrier weighting yields information on the carrier frequency offset  $\theta_e$  as well. For general  $w[k]$  and  $n_e \in \mathbb{Z}$ , we obtain

$$c_r[n, \tau] = \sigma_c^2 e^{j2\pi\theta_e\tau} \Gamma_M[\tau] a_M^{(\tau)}[n - n_e] + c_\rho[\tau]. \quad (12)$$

If  $w[k]$  is chosen such that  $\Gamma_M[\tau] \neq 0$  for at least one  $\tau \in [1, M-1]$ ,  $c_r[n, \tau]$  contains information on the parameter  $\theta_e$  as well. Note that  $c_r[n, \tau] = c_\rho[\tau]$  for  $|\tau| \geq M$ . Again, similar expressions can be given for the more general case  $n_e \in \mathbb{R}$ . The use of overlapping filters (i.e.,  $g[n]$  is longer than  $M$  samples) would also introduce cyclostationarity in the OFDM signal. However, it is well known from filter bank theory that such filters do not allow perfect reconstruction (orthogonality or biorthogonality) for  $N = M$  [21]. Therefore, this case will not be investigated.

**CP OFDM Systems:** Let us next consider OFDM systems employing a CP [2]. Here,  $M = N + P$ , where  $P$  denotes the length of the CP, and

$$g[n] = \begin{cases} \frac{1}{\sqrt{N}}, & n = 0, 1, \dots, M-1 \\ 0, & \text{else,} \end{cases}$$

and

$$h[n] = \begin{cases} \frac{1}{\sqrt{N}}, & n = 0, 1, \dots, N-1 \\ 0, & \text{else.} \end{cases}$$

For the sake of simplicity, we assume that  $P \leq N$  (i.e., the length of the CP is at most 50% of the symbol length). For  $n_e \in \mathbb{Z}$ , we obtain

$$c_r[n, \tau] = \sigma_c^2 e^{j2\pi\theta_e\tau} \Gamma_N[\tau] a_M^{(\tau)}[n - n_e] + c_\rho[\tau].$$

<sup>5</sup>Recall that  $\Gamma_M[\tau]$  is  $M$ -periodic.

<sup>6</sup>By pulse shaping, we mean that  $g[n]$  is not equal to the rectangular function on the interval  $[0, M-1]$ .

Note that  $c_r[n, \tau]$  contains information on the synchronization parameters for all  $\tau$  satisfying  $\Gamma_N[\tau] \neq 0$  and  $1 \leq |\tau| \leq M-1$ . Similar expressions can be given for the more general case  $n_e \in \mathbb{R}$ . If no subcarrier weighting is employed,  $\Gamma_N[\tau] = N \sum_{s=-\infty}^{\infty} \delta[\tau - sN]$  and  $c_r[n, \tau]$  contains information on the synchronization parameters for  $\tau = \pm N$  only. Hence, the use of subcarrier weighting yields more samples of  $c_r[n, \tau]$  containing information on the synchronization parameters  $n_e$  and  $\theta_e$ . Later, we will show that this improves estimation accuracy.

**Time-Frequency Guard Regions and Pulse Shaping:** For the general case of OFDM with time-frequency guard regions (i.e.,  $M > N$ ), overlapping pulse shaping filters  $g[n]$  satisfying perfect reconstruction (orthogonality or biorthogonality) are possible. Here, cyclostationarity is caused by the time-frequency guard regions and by the overlapping nature of the pulse shaping filter. Let us specialize (10) for this case. For  $n_e \in \mathbb{Z}$  without subcarrier weighting, we obtain

$$c_r[n, \tau] = \begin{cases} \sigma_c^2 N a_M^{(0)}[n - n_e] + c_\rho[0], & \tau = 0 \\ \sigma_c^2 N e^{j2\pi\theta_e s N} a_M^{(sN)}[n - n_e] + c_\rho[sN], & \tau = sN, s \in [-L, L] \\ c_\rho[\tau], & \text{else} \end{cases}$$

where  $L = \lfloor (L_g - 1)/N \rfloor$  with  $L_g$  denoting the length of the pulse shaping filter  $g[n]$ . Again, for arbitrary  $n_e \in \mathbb{R}$ , similar expressions for  $c_r[n, \tau]$  are obtained from (9). If subcarrier weighting is employed,  $c_r[n, \tau]$  will contain information on the synchronization parameters for all<sup>7</sup>  $\tau$  satisfying  $\Gamma_N[\tau] \neq 0$  and  $|\tau| \leq L_g - 1$ , which in turn improves estimation accuracy (to be shown in Section IV).

## B. Cyclostationarity in OFDM/OQAM Systems

We shall next establish cyclostationarity of pulse shaping OFDM/OQAM signals with  $N = M$  (i.e., no guard regions). Using (8) and (5), a derivation similar to the one provided in the Appendix reveals that the correlation function of  $r[n]$  is given by

$$\begin{aligned} c_r[n, \tau] &= e^{j2\pi\theta_e\tau} \Gamma_M[\tau] \\ &\cdot \left[ \frac{\sigma_{c,R}^2}{M} \sum_{l=-\infty}^{\infty} g[l]g[l-\tau] \sum_{s=0}^{M-1} e^{-j2\pi(s/M)(l-n+n_e)} \right. \\ &\quad \left. + \frac{\sigma_{c,I}^2}{M} \sum_{l=-\infty}^{\infty} g[l]g[l-\tau] \right. \\ &\quad \left. \cdot \sum_{s=0}^{M-1} \exp\left(-j2\pi \frac{s}{M} \left(l-n+n_e - \frac{M}{2}\right)\right) \right] + c_\rho[\tau] \end{aligned} \quad (13)$$

for  $n_e \in \mathbb{R}$ . Again, for  $n_e \in \mathbb{Z}$ , (13) can be further simplified. We omit the expression. Using (13), it is easily verified that  $c_r[n + M, \tau] = c_r[n, \tau]$ . Thus, the underlying signal  $r[n]$  is indeed CS with period  $M$ .

If no pulse shaping and no subcarrier weighting is employed, i.e.,  $g[n] = (1/\sqrt{M})$  for  $n \in [0, M-1]$  and 0 else, and

<sup>7</sup>For  $\tau = 0$  the correlation function  $c_r[n, \tau]$  contains information on  $n_e$  only.

$|w[k]| = 1$  for  $k = 0, 1, \dots, M-1$ , it is easily seen that  $r[n]$  is stationary and does not contain information on the synchronization parameters. Just like in the OFDM/QAM case, subcarrier weighting introduces cyclostationarity in the OFDM signal such that the second-order statistics of  $r[n]$  contain information on the synchronization parameters  $n_e$  and  $\theta_e$ .

If pulse shaping is employed (i.e., the filter  $g[n]$  is longer than the symbol period) and no subcarrier weighting is used, we have

$$c_r[n, \tau] = \begin{cases} M \left[ \sigma_{c,R}^2 a_M^{(0)}[n-n_e] \right. \\ \left. + \sigma_{c,I}^2 a_M^{(0)} \left[ n + \frac{M}{2} - n_e \right] \right] + c_\rho[0], & \tau = 0 \\ M e^{j2\pi\theta_e s M} \left[ \sigma_{c,R}^2 a_M^{(sM)}[n-n_e] \right. \\ \left. + \sigma_{c,I}^2 a_M^{(sM)} \left[ n + \frac{M}{2} - n_e \right] \right] \\ \left. + c_\rho[sM], \right. & \tau = sM, \\ & s \in [-L, L] \\ c_\rho[\tau], & \text{else} \end{cases}$$

for  $n_e \in \mathbb{Z}$  and  $L = \lfloor (L_g - 1/N) \rfloor$  with  $L_g$  denoting the length of the filter  $g[n]$ . If subcarrier weighting is used, the correlation function  $c_r[n, \tau]$  will contain information on the synchronization parameters<sup>8</sup> for all  $\tau$  satisfying  $\Gamma_M[\tau] \neq 0$  and  $|\tau| \leq L_g - 1$ .

We conclude this section by noting that it is remarkable that pulse shaping OFDM/OQAM signals are CS although no guard interval is used. We note, however, that for a given average transmit power, the use of pulse shaping, subcarrier weighting, or periodic precoding leads to a reduction in the effective minimum constellation distance, and hence in order to achieve a given bit-error rate, a higher average transmit power is required. Therefore, even though the transmission rate is kept constant, a loss in spectral efficiency is incurred.

#### IV. BLIND ESTIMATION OF SYNCHRONIZATION PARAMETERS

Based on the results of the previous section, we shall next provide algorithms for the blind estimation of the synchronization parameters  $n_e$  and  $\theta_e$ .

##### A. Blind Estimation

*Fourier Series Expansion of the Correlation Function:* From (9) and (13), it follows that the correlation function  $c_r[n, \tau]$  of the received signal  $r[n]$  is  $M$ -periodic in  $n$ . For a fixed lag  $\tau$ ,  $c_r[n, \tau]$  can therefore be expanded into a Fourier series with Fourier coefficients given by

$$C_r[k, \tau] = \frac{1}{M} \sum_{n=0}^{M-1} c_r[n, \tau] e^{-j(2\pi/M)kn}, \quad k = 0, 1, \dots, M-1.$$

<sup>8</sup>For  $\tau = 0$ , the correlation function  $c_r[n, \tau]$  contains information on  $n_e$  only.

It is shown in the Appendix that

$$C_r[k, \tau] = \frac{\sigma_c^2}{M} e^{j2\pi\theta_e\tau} e^{-j(2\pi/M)kn_e} \Gamma_N[\tau] A^{(g,g)} \left[ \tau, \frac{k}{M} \right] + c_\rho[\tau] \delta[k], \quad k = 0, 1, \dots, M-1. \quad (14)$$

in the OFDM/QAM case. Similarly, in the OFDM/OQAM case, it can be shown that

$$C_r[k, \tau] = \frac{1}{M} e^{j2\pi\theta_e\tau} e^{-j(2\pi/M)kn_e} \Gamma_M[\tau] A^{(g,g)} \left[ \tau, \frac{k}{M} \right] \cdot [\sigma_{c,R}^2 + (-1)^k \sigma_{c,I}^2] + c_\rho[\tau] \delta[k], \quad k = 0, 1, \dots, M-1. \quad (15)$$

Since  $\sigma_c^2$ ,  $\sigma_{c,R}^2$ ,  $\sigma_{c,I}^2$ ,  $g[n]$ ,  $w[k]$ , and hence  $\Gamma_N[\tau]$  are known in the receiver, in the OFDM/QAM case their influence can be eliminated by defining

$$C[k, \tau] = \begin{cases} \frac{C_r[k, \tau]}{\frac{\sigma_c^2}{M} \Gamma_N[\tau] A^{(g,g)} \left[ \tau, \frac{k}{M} \right]}, & [k, \tau] \in \mathcal{I} \\ 0, & \text{else} \end{cases} \quad (16)$$

where<sup>9</sup>  $\mathcal{I} := \{[k, \tau] | \Gamma_N[\tau] A^{(g,g)}[\tau, k/M] \neq 0\}$ . In the OFDM/OQAM case, we can define similarly

$$C[k, \tau] = \begin{cases} \frac{C_r[k, \tau]}{\frac{1}{M} \Gamma_M[\tau] A^{(g,g)} \left[ \tau, \frac{k}{M} \right] [\sigma_{c,R}^2 + (-1)^k \sigma_{c,I}^2]}, & [k, \tau] \in \mathcal{I} \\ 0, & \text{else} \end{cases} \quad (17)$$

where  $\mathcal{I} := \{[k, \tau] | \Gamma_M[\tau] A^{(g,g)}[\tau, k/M] [\sigma_{c,R}^2 + (-1)^k \sigma_{c,I}^2] \neq 0\}$ . We therefore have

$$C[k, \tau] = e^{j2\pi\theta_e\tau} e^{-j(2\pi/M)kn_e} + \frac{c_\rho[\tau]}{\frac{\sigma_c^2}{M} \Gamma_N[\tau] A^{(g,g)} \left[ \tau, \frac{k}{M} \right]} \delta[k] \quad (18)$$

for  $[k, \tau] \in \mathcal{I}$  in the OFDM/QAM case and

$$C[k, \tau] = e^{j2\pi\theta_e\tau} e^{-j(2\pi/M)kn_e} + \frac{c_\rho[\tau]}{\frac{1}{M} \Gamma_M[\tau] A^{(g,g)} \left[ \tau, \frac{k}{M} \right] [\sigma_{c,R}^2 + (-1)^k \sigma_{c,I}^2]} \delta[k] \quad (19)$$

for  $[k, \tau] \in \mathcal{I}$  in the OFDM/OQAM case. From (18) and (19), it follows that the impact of stationary noise on the estimator

<sup>9</sup>Since  $C[k, \tau]$  is  $M$ -periodic in  $k$ , in the following we consider  $k \in [0, M-1]$  only.

is minimized by considering  $\mathcal{C}[k, \tau]$  for  $k \in [1, M-1]$  only. In practice, it is desirable to have as many samples of  $\mathcal{C}[k, \tau]$  containing information on the synchronization parameters as possible. The subcarrier weighting function  $w[k]$  and the pulse shaping filter  $g[n]$  should therefore be chosen such that the product  $\Gamma_N[\tau]A^{(g,g)}[\tau, k/M]$  in the OFDM/QAM case and  $\Gamma_M[\tau]A^{(g,g)}[\tau, k/M][\sigma_{c,R}^2 + (-1)^k\sigma_{c,I}^2]$  in the OFDM/OQAM case has as few zeros as possible. We shall see later that these zeros determine the estimators' accuracy and acquisition range. Note, however, that due to the (bi)orthogonality conditions (2) and (4) the ambiguity function  $A^{(g,g)}[k, \theta]$  vanishes on a lattice determined by the parameters  $M$  and  $N$ . These zeros cannot be avoided.

*Estimation Algorithms:* Now, following a procedure first suggested by Gini and Giannakis for single-carrier systems [1], the carrier frequency offset can be retrieved from  $\mathcal{C}[k, \tau]$  as

$$\theta_e = \frac{\arg\{\mathcal{C}[k, \tau]\mathcal{C}[M-k, \tau]\}}{4\pi\tau}, \quad [k, \tau] \in \mathcal{I} \quad (20)$$

where  $\arg$  denotes the unwrapped phase,  $\tau \neq 0$ , and  $k \in [1, M-1]$ . If  $[k, \tau] \in \mathcal{I}$ , it follows from<sup>10</sup>  $A^{(g,g)*}[\tau, k/M] = A^{(g,g)}[\tau, (M-k)/M]$  that  $[M-k, \tau] \in \mathcal{I}$  as well. Note that estimation of  $\theta_e$  according to (20) will in general require phase unwrapping. Given the carrier frequency offset  $\theta_e$ , the timing error can be obtained from (18) as

$$n_e = -\frac{M}{2\pi k} \arg\{\mathcal{C}[k, \tau]e^{-j2\pi\theta_e\tau}\}, \quad [k, \tau] \in \mathcal{I} \quad (21)$$

where  $k \in [1, M-1]$  was assumed. Estimation of  $n_e$  using (21) will in general also require phase unwrapping.

*Carrier Frequency Acquisition Range:* From (20), it follows that in order to avoid ambiguity in the estimation of  $\theta_e$ , we have to require

$$|4\pi\tau_{\min}\theta_e| < \pi \quad (22)$$

where  $\tau_{\min}$  is the smallest  $\tau \geq 1$  such that  $[k, \tau] \in \mathcal{I}$  for some  $k \in [1, M-1]$ . From  $\Gamma_N[-\tau] = \Gamma_N^*[\tau]$  and  $A^{(g,g)}[-\tau, \theta] = e^{j2\pi\tau\theta}A^{(g,g)}[\tau, \theta]$ , it follows that  $[k, \tau] \in \mathcal{I}$  implies that  $[k, -\tau] \in \mathcal{I}$ . It is therefore not necessary to distinguish between negative and positive  $\tau$  in this context. Provided that  $\tau_{\min} = 1$ , the maximum allowed frequency offset follows from (22) as  $|\theta_e| < 1/4$ , i.e., the carrier frequency acquisition range is half the bandwidth of the OFDM signal. We shall see later that if no subcarrier weighting is used  $\tau_{\min} \geq N$  and hence  $|\theta_e| < 1/(4N)$ . We therefore conclude that it is important to choose  $w[k]$  such that  $\tau_{\min}$  is as small as possible.

*Symbol Timing Acquisition Range:* From (21), it follows that unambiguous estimation of the timing error  $n_e$  is possible if

$$\left| \frac{2\pi k_{\min}}{M} n_e \right| < \pi$$

where  $k_{\min}$  is the smallest  $k \in [1, M-1]$  such that  $[k, \tau] \in \mathcal{I}$  for some  $\tau$ . Assuming that  $k_{\min} = 1$ , we get  $|n_e| < M/2$ . The symbol timing acquisition range is therefore one symbol

<sup>10</sup>Recall that  $g[n]$  was assumed to be real-valued.

interval. We shall see later how the use of periodic transmitter precoding increases the length of the symbol timing acquisition range.

*The Cyclic Spectrum Approach:* We shall next present an alternative method for estimating  $n_e$  and  $\theta_e$  from the second-order cyclic statistics of  $r[n]$ . This approach *avoids phase unwrapping and allows a full range carrier frequency acquisition* (i.e.,  $|\theta_e| < 1/2$ ). In the following, we shall need the cyclic spectrum which is defined as the Fourier transform of  $\mathcal{C}[k, \tau]$  with respect to  $\tau$ , i.e.,

$$S[k, f] = \sum_{\tau=-\infty}^{\infty} \mathcal{C}[k, \tau]e^{-j2\pi\tau f}.$$

From (18), we obtain

$$S[k, f] = e^{-j(2\pi/M)kn_e} \frac{\sin\left(2\pi(\theta_e - f)\left(L_\tau + \frac{1}{2}\right)\right)}{\sin(\pi(\theta_e - f))}$$

for  $k \in [1, M-1]$  and  $[k, \tau] \in \mathcal{I}$  for  $|\tau| \leq L_\tau$  with  $L_\tau$  denoting the maximum  $\tau$  satisfying  $[k, \tau] \in \mathcal{I}$ . The carrier frequency offset can be obtained from the magnitude of the cyclic spectrum as

$$\theta_e = \arg \max_{|f| < 1/2} |S[k, f]|. \quad (23)$$

From (23), it follows that  $\theta_e$  can be estimated unambiguously if  $|\theta_e| < 1/2$ , which means that the carrier frequency acquisition range is the *entire bandwidth* of the OFDM signal. We note that using (23), the estimation of the carrier frequency offset reduces to the estimation of the frequency of a CISOID, which can be accomplished using one of the standard frequency estimation algorithms discussed for example in [22]. Finally, the timing offset can be retrieved from the cyclic spectrum as

$$n_e = -\frac{M}{2\pi k} \arg\{S[k, f]\} \quad (24)$$

where  $f$  has to be chosen such that

$$\frac{\sin\left(2\pi(\theta_e - f)\left(L_\tau + \frac{1}{2}\right)\right)}{\sin(\pi(\theta_e - f))} > 0$$

and  $k \in [1, M-1]$ . We shall see later that in practice taking  $f$  to be the estimate of  $\theta_e$  is a good choice.

Assuming that no subcarrier weighting is employed and  $k \in [1, M-1]$  is such that  $[k, \tau] \in \mathcal{I}$  for  $\tau = sN$  with  $s \in \mathbb{Z}$ , the cyclic spectrum is given by

$$S[k, f] = e^{-j(2\pi/M)kn_e} \frac{1}{N} \sum_{l=0}^{N-1} \frac{\sin\left(2\pi\left(\theta_e - \left(f - \frac{l}{N}\right)\right)\left(L_\tau + \frac{1}{2}\right)\right)}{\sin\left(\pi\left(\theta_e - \left(f - \frac{l}{N}\right)\right)\right)}$$

which shows that using the cyclic spectrum approach unambiguous estimation of the carrier frequency offset is possible for  $|\theta_e| < 1/(2N)$ . We conclude again that the use of subcarrier weighting is crucial for increasing the carrier frequency acquisition range.

*Estimation in Presence of a Time-Dispersive Channel:* So far, we neglected the influence of time-dispersive channels. We shall next adapt our estimators to time-dispersive environments. For the sake of simplicity, we consider the OFDM/QAM case only. Assuming that the received signal is given by  $r[n] = e^{j(2\pi\theta_e n + \phi)}(x * b)[n - n_e] + \rho[n]$  where  $b[n]$  denotes the known channel impulse response, it is tedious but straightforward to show that

$$C_r[k, \tau] = \frac{\sigma_c^2}{M} e^{j2\pi\theta_e \tau} e^{-j(2\pi/M)kn_e} \hat{A}^{(g,b)}\left[\tau, \frac{k}{M}\right] + c_\rho[\tau]\delta[k]$$

where

$$\begin{aligned} \hat{A}^{(g,b)}[\tau, \theta] &= \sum_s b[s] \sum_l b[l - \tau] \Gamma_N[l - s] \\ &\cdot \sum_n g[n - s] g[n - l] e^{-j2\pi n \theta}. \end{aligned}$$

Since the channel impulse response  $b[n]$ , the transmitter pulse shaping filter  $g[n]$ , and  $\sigma_c^2$  are known at the receiver, we can define

$$C[k, \tau] = \begin{cases} \frac{C_r[k, \tau]}{\frac{\sigma_c^2}{M} \hat{A}^{(g,b)}\left[\tau, \frac{k}{M}\right]}, & [k, \tau] \in \mathcal{I} \\ 0, & \text{else} \end{cases} \quad (25)$$

where  $\mathcal{I} := \{[k, \tau] | \hat{A}^{(g,b)}[\tau, k/M] \neq 0\}$ . Consequently

$$C[k, \tau] = e^{j2\pi\theta_e \tau} e^{-j(2\pi/M)kn_e} + \frac{c_\rho[\tau]}{\frac{\sigma_c^2}{M} \hat{A}^{(g,b)}\left[\tau, \frac{k}{M}\right]} \delta[k]$$

for  $[k, \tau] \in \mathcal{I}$ . Finally,  $n_e$  and  $\theta_e$  can be retrieved from  $C[k, \tau]$  using (20) and (21) or (23) and (24), respectively. The effect of the time-dispersive channel has therefore been “divided out.” Note, however, that the channel  $b[n]$  influences  $\mathcal{I}$  and consequently the estimators’ accuracy and acquisition range. The impact of  $\mathcal{I}$  on the estimators’ accuracy will be discussed in Section IV-C. The performance of our estimators in the presence of an unknown time-dispersive channel will be studied in Section V through simulations.

### B. Increasing the Symbol Timing Acquisition Range

We have seen in Section IV-A that the acquisition range of the symbol timing estimators (21) and (24) is one symbol length, i.e.,  $M$  samples. In practice, in many applications it is desirable to have a greater timing acquisition range in order to avoid an

initial rough acquisition step. We shall next propose a specific form of periodic transmitter precoding, which yields a symbol timing acquisition range of in principle arbitrary length.

In order to simplify the presentation, we shall restrict our discussion to the OFDM/QAM case with  $n_e \in \mathbb{Z}$ . Assume that the symbol sequences  $c_{k,l}$  on each subcarrier (i.e., for each value of  $k$ ) are multiplied by the same periodic *nonconstant-modulus* sequence  $a[l]$  with period  $P$ , i.e.,  $a[l + P] = a[l]$ . The corresponding transmit signal (taking into account subcarrier weighting as well) reads

$$x[n] = \sum_{k=0}^{N-1} \sum_{l=-\infty}^{\infty} c_{k,l} w[k] a[l] g[n - lM] e^{j(2\pi/N)k(n-lM)}.$$

Using arguments along the lines of the proof in the Appendix, the correlation function of the received signal  $r[n] = e^{j(2\pi\theta_e n + \phi)} x[n - n_e]$  is obtained as

$$\begin{aligned} c_r[n, \tau] &= \sigma_c^2 \Gamma_N[\tau] e^{j2\pi\theta_e \tau} \sum_{l=-\infty}^{\infty} |a[l]|^2 g[n - n_e - lM] \\ &\cdot g[n - n_e - lM - \tau] + c_\rho[\tau]. \end{aligned} \quad (26)$$

From the  $P$ -periodicity of  $a[l]$ , it follows that  $c_r[n, \tau]$  is  $PM$ -periodic with respect to  $n$  for all  $\tau$ , which implies that  $r[n]$  is CS with period  $PM$ . We note that it is important to choose the precoding sequence  $a[l]$  to be nonconstant-modulus. Otherwise,  $c_r[n, \tau]$  will be  $M$ -periodic rather than  $PM$ -periodic and the symbol timing acquisition range is not increased. The Fourier series coefficients of  $c_r[n, \tau]$  with respect to  $n$  are obtained as

$$\begin{aligned} C_r[k, \tau] &= \frac{\sigma_c^2}{PM} \Gamma_N[\tau] e^{j2\pi\theta_e \tau} e^{-j(2\pi/PM)kn_e} \Phi_P[k] \\ &\cdot A^{(g,g)}\left[\tau, \frac{k}{PM}\right] + c_\rho[\tau]\delta[k] \end{aligned} \quad (27)$$

where  $\Phi_P[k] = \sum_{i=0}^{P-1} |a[i]|^2 e^{-j(2\pi/P)ki}$  is the  $P$ -point DFT of  $|a[i]|^2$ . Now, we can define

$$\begin{aligned} C[k, \tau] &= \begin{cases} \frac{C_r[k, \tau]}{\frac{\sigma_c^2}{PM} \Gamma_N[\tau] \Phi_P[k] A^{(g,g)}\left[\tau, \frac{k}{PM}\right]}, & [k, \tau] \in \mathcal{I} \\ 0, & \text{else} \end{cases} \end{aligned}$$

where  $\mathcal{I} := \{[k, \tau] | \Gamma_N[\tau] \Phi_P[k] A^{(g,g)}[\tau, k/PM] \neq 0\}$ . Consequently

$$\begin{aligned} C[k, \tau] &= e^{j2\pi\theta_e \tau} e^{-j(2\pi/PM)kn_e} \\ &+ \frac{c_\rho[\tau]}{\frac{\sigma_c^2}{PM} \Gamma_N[\tau] \Phi_P[k] A^{(g,g)}\left[\tau, \frac{k}{PM}\right]} \delta[k]. \end{aligned} \quad (28)$$

The influence of stationary noise can be minimized by considering  $C[k, \tau]$  for  $k \in [1, PM - 1]$  only. The carrier frequency offset can now be obtained from (28) as

$$\theta_e = \frac{\arg\{C[k, \tau]C[PM - k, \tau]\}}{4\pi\tau}, \quad [k, \tau] \in \mathcal{I} \quad (29)$$

where  $k \in [1, PM - 1]$  was assumed. The timing error  $n_e$  can be estimated as

$$n_e = -\frac{PM}{2\pi k} \arg\{C[k, \tau]e^{-j2\pi\theta_e\tau}\} \quad (30)$$

which shows that now unambiguous estimation of  $n_e$  is possible if

$$\left| \frac{2\pi k_{\min} n_e}{PM} \right| < \pi$$

where  $k_{\min}$  is the smallest  $k \in [1, PM - 1]$  such that  $[k, \tau] \in \mathcal{I}$  for some  $\tau$ . Assuming that  $k_{\min} = 1$ , we get  $|n_e| < (PM/2)$ . Therefore,  $P$  determines the symbol timing acquisition range, which obviously can be made arbitrarily large.

### C. Estimators and Estimation of Cyclic Statistics

We shall next discuss the estimation of the cyclic statistics  $C_r[k, \tau]$ , and then provide estimators for the synchronization parameters based on the estimated Fourier series coefficients  $\hat{C}_r[k, \tau]$ .

*Estimation of Cyclic Statistics:* In practice, the cyclic statistics  $C_r[k, \tau]$  can be estimated from a finite data record  $\{r[n]\}_{n=0}^{L-1}$  of length  $L$  according to [14], [1]

$$\hat{C}_r[k, \tau] = \frac{1}{L} \sum_{n=0}^{L-1} r[n]r^*[n - \tau]e^{-j(2\pi/M)kn}. \quad (31)$$

If periodic transmitter precoding (as described in Section IV-B) is employed using a precoding sequence with period  $P$ , (31) has to be replaced by

$$\hat{C}_r[k, \tau] = \frac{1}{L} \sum_{n=0}^{L-1} r[n]r^*[n - \tau]e^{-j(2\pi/PM)kn}. \quad (32)$$

If the noise process  $\rho[n]$  satisfies the so-called mixing conditions<sup>11</sup> [23], [24], the estimators in (31) and (32) are asymptotically unbiased and mean-square-sense consistent [1].

*Estimators:* We are now ready to provide estimators for  $n_e$  and  $\theta_e$  based on the estimated cyclic statistics  $\hat{C}_r[k, \tau]$ . In practice, it is desirable to average over  $\mathcal{I}$  (this potentially reduces the effects of pattern and additive noise), or more specifically<sup>12</sup>

$$\hat{\theta}_e = \frac{1}{4\pi|\mathcal{I}'|} \sum_{[k, \tau] \in \mathcal{I}'} \frac{1}{\tau} \arg\{\hat{C}[k, \tau]\hat{C}[M - k, \tau]\} \quad (33)$$

$$\hat{n}_e = -\frac{M}{2\pi|\mathcal{I}''|} \sum_{[k, \tau] \in \mathcal{I}''} \frac{1}{k} \arg\{\hat{C}[k, \tau]e^{-j2\pi\hat{\theta}_e\tau}\} \quad (34)$$

<sup>11</sup>The mixing conditions are satisfied by all finite memory signals in practice.

<sup>12</sup>If transmitter precoding is employed the expressions provided in (33) and (34) have to be modified according to (29) and (30).

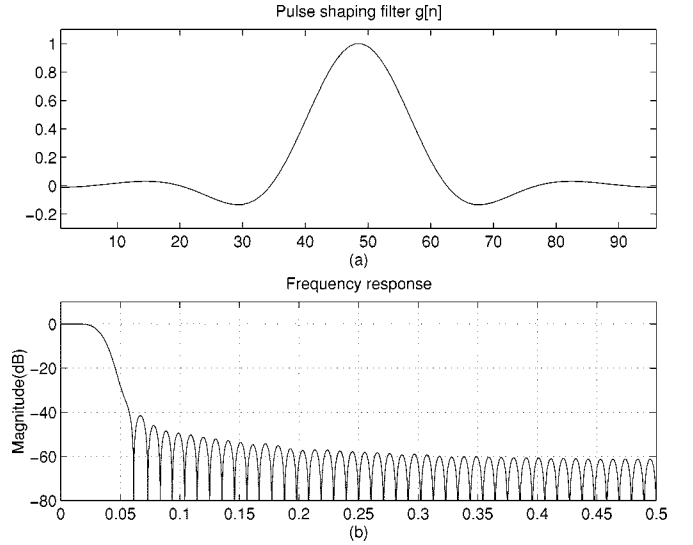


Fig. 1. Pulse shaping filter used in the simulation examples: (a) impulse response and (b) transfer function.

where  $\hat{C}[k, \tau]$  is obtained by replacing  $C_r[k, \tau]$  in (16) by  $\hat{C}_r[k, \tau]$ ,  $\mathcal{I}' = \mathcal{I} \setminus \{k = 0\} \setminus \{\tau = 0\}$  (i.e., the set  $\mathcal{I}$  except for the  $k = 0$  axis and the  $\tau = 0$  axis), and  $\mathcal{I}'' = \mathcal{I} \setminus \{k = 0\}$ . From (33) and (34), it follows that it is desirable to have as many samples of  $C[k, \tau]$  containing information on the synchronization parameters as possible, since this allows more averaging and therefore in general increases the estimation accuracy. Since  $\hat{C}_r[k, \tau]$  is an asymptotically unbiased and consistent estimator of  $C_r[k, \tau]$ , it follows that  $\hat{n}_e$  and  $\hat{\theta}_e$  are asymptotically unbiased and consistent estimators of  $n_e$  and  $\theta_e$ .

Estimators based on the cyclic spectrum can be obtained from (23) and (24) as

$$\hat{\theta}_e = \frac{1}{M-1} \sum_{k=1}^{M-1} \arg \max_{|f| < 1/2} |\hat{S}[k, f]| \quad (35)$$

$$\hat{n}_e = -\frac{M}{2\pi(M-1)} \sum_{k=1}^{M-1} \frac{1}{k} \arg\{\hat{S}[k, f]\} \quad (36)$$

where  $\hat{S}[k, f]$  is obtained by windowing  $\hat{C}[k, \tau]$  with  $W[\tau]$  supported in  $|\tau| \leq L_w \leq L_\tau$  and taking the Fourier transform as [1]

$$\hat{S}[k, f] = \sum_{\tau=-L_w}^{L_w} \hat{C}[k, \tau]W[\tau]e^{-j2\pi\tau f}.$$

Since  $S[k, f]$  exhibits a  $(\sin f)/f$  behavior around  $\theta_e$ , a good choice will be to take  $f = \hat{\theta}_e$ .

## V. SIMULATION RESULTS

In this section, we provide simulation results demonstrating the performance of the proposed estimators. Unless stated otherwise, we simulated a pulse shaping OFDM/QAM system with time-frequency guard region,  $N = 8$  channels, symbol length  $M = 16$ , and filter length 96 (see Fig. 1). The data

<sup>13</sup>For  $\theta_e = 0$  the MSE of  $\hat{\theta}_e$  was in the order of MATLAB's computational accuracy.



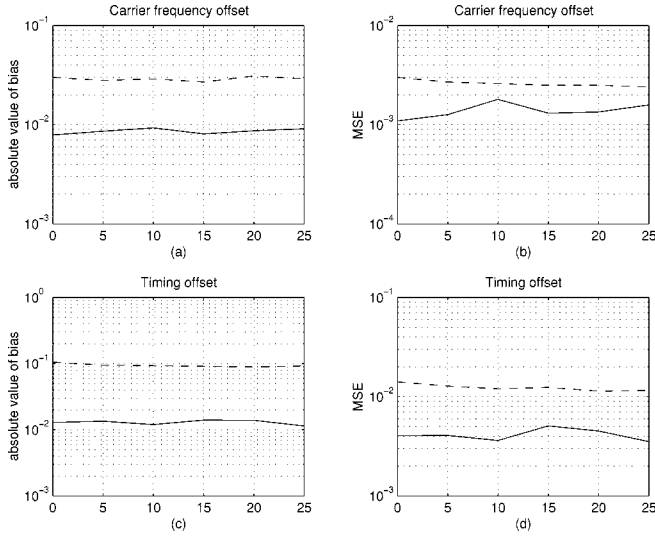


Fig. 2. Bias and MSE of carrier frequency and symbol timing offset estimators (33) and (34), respectively, versus SNR/decibel for  $n_e = 2$  and  $\theta_e = 0.0625$  (solid curves correspond to AWGN case and dashed curves correspond to multipath case). (a) Bias and (b) MSE of  $\hat{\theta}_e$  versus  $\theta_e$ . (c) Bias and (d) MSE of  $\hat{n}_e/M$  versus  $n_e/M$ .

symbols were independent and identically distributed 4-PSK symbols with  $\sigma_c^2 = 2$ . The signal-to-noise-ratio (SNR) was defined as  $\text{SNR} = \sigma_c^2/\sigma_p^2$ , where  $\sigma_p^2$  is the variance of the white noise process  $p[n]$ . All results were obtained by averaging over 200 independent Monte Carlo trials. Each realization consisted of 1024 data symbols (i.e., 128 OFDM symbols). Furthermore, in all simulation examples except for the last one, the estimates of the cyclic statistics  $\hat{C}_\tau[k, \tau]$  were obtained using the entire data record. The subchannel weighting vector was chosen as  $\mathbf{w} = [1.1 \ 2.0 \ 1.4 \ 1.33 \ 1.0 \ 0.6 \ 0.8 \ 1.2]$ . Note that this choice satisfies  $\Gamma_N[\tau] \neq 0$  for  $\tau \in [0, N-1]$ .

**Simulation Example 1:** In the first simulation example, we computed the bias and the mean square error (MSE) of the carrier frequency offset estimator (33) and the timing offset estimator (34) for  $n_e = 2$  and  $\theta_e = 0.0625$  (i.e., half the subcarrier spacing) for the AWGN case (solid curves) and in the presence of an unknown four-tap multipath channel. We averaged over  $\{[1, \tau] | 1 \leq \tau \leq 24\}$ . Fig. 2(a) and (b) shows the bias and the MSE, respectively, of  $\hat{\theta}_e$  versus  $\theta_e$  as a function of SNR in decibels. Fig. 2(c) and (d) shows the bias and the MSE, respectively, of  $\hat{n}_e/M$  versus  $n_e/M$  as a function of SNR. In the AWGN case, our estimators perform well even for SNR values as small as 0 dB. However, it has to be noted that the performance does not improve with increasing SNR. We can furthermore see that the presence of an unknown multipath channel leads to a degradation in the estimator performance.

**Simulation Example 2:** In the second simulation example (see Fig. 3), we computed the bias and the MSE of the carrier frequency offset estimator (33) at an SNR of 9 dB as a function of the carrier frequency offset.<sup>14</sup> Again, we averaged over the interval  $\{[1, \tau] | 1 \leq \tau \leq 24\}$ . Fig. 3 shows that the performance of the estimator improves for smaller values of  $\theta_e$ .

<sup>14</sup>Recall that the acquisition range of the estimator (33) is restricted to  $|\theta_e| < 1/4$ . For  $|\theta_e|$  close to  $1/4$ , however, the estimator becomes inaccurate. We therefore simulated the range  $|\theta_e| \leq 0.2$  only.

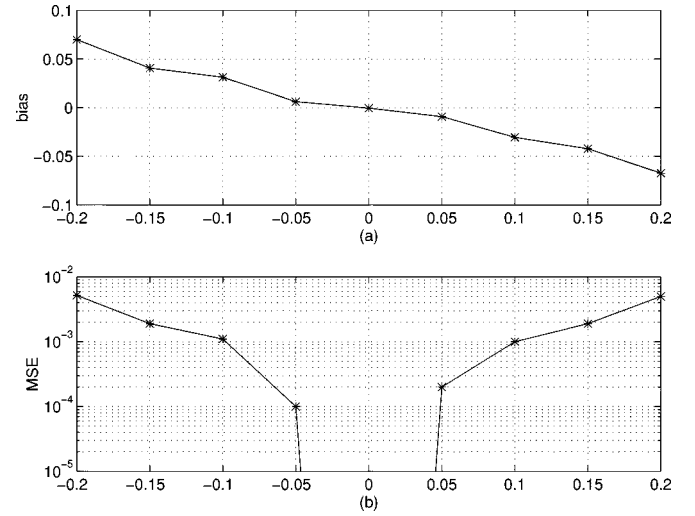


Fig. 3. (a) Bias and (b) MSE<sup>13</sup> of  $\hat{\theta}_e$  according to (33) versus  $\theta_e$  as a function of  $\theta_e$ .

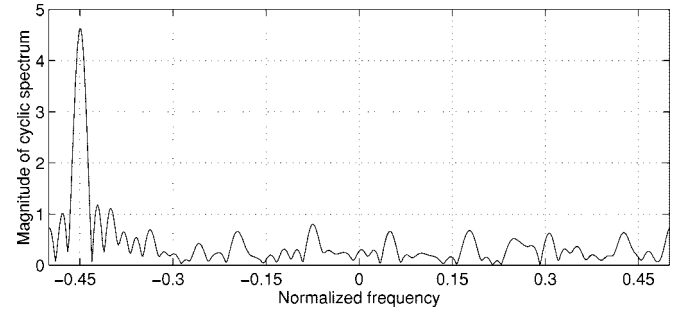


Fig. 4. Magnitude of the cyclic spectrum  $\hat{S}[1, f]$ .

**Simulation Example 3:** In this simulation example, we consider estimation of the carrier frequency offset using the cyclic spectrum approach. Fig. 4 shows  $|\hat{S}[1, f]|$  for  $\theta_e = -0.45$ . It is clearly seen that  $\hat{S}[1, f]$  exhibits a peak at the carrier frequency offset.

**Simulation Example 4:** We shall next demonstrate that our method is capable of estimating noninteger values of  $n_e$ . For  $n_e = 8/3$  and  $\theta_e = 0.04$ , using the estimators (33) and (34), Fig. 5(a) and (b) shows the bias and the MSE, respectively, of  $\hat{\theta}_e$  versus  $\theta_e$  as a function of the SNR in decibels. Fig. 5(c) and (d) shows the bias and the MSE, respectively, of  $\hat{n}_e/M$  versus  $(n_e/M)$  as a function of the SNR in decibels. The timing offset estimate has been obtained by averaging over  $\{[1, \tau] | 0 \leq \tau \leq 10\}$ , and the carrier frequency offset estimator used the samples  $[k, \tau]$  with  $k = 0, 1$  and  $1 \leq \tau \leq 19$ . The fractional delay has been introduced by interpolating the signal  $x[n]$  by a factor of 3, shifting the interpolated signal by eight samples, and decimating the result by a factor of 3.

**Simulation Example 5:** In this example, we compared the performance of the timing offset estimator proposed in [13] (VSB-estimator) to the estimator (34) (CS-estimator). We simulated a CP OFDM system with  $N = 8$ , a CP of length 8 (i.e.,  $M = 16$ ),  $\theta_e = 0$ , and  $n_e = 2$ . Fig. 6(a) and (b) shows the bias and the MSE, respectively, of  $\hat{n}_e/M$  versus  $(n_e/M)$  as a function of SNR in decibels. We can see that our estimator outperforms the VSB-estimator in the below 10–15-dB SNR regime.

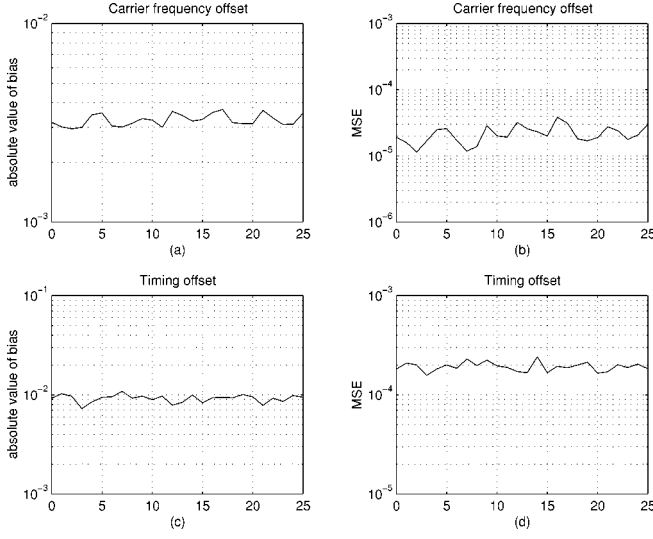


Fig. 5. Bias and MSE of carrier frequency and symbol timing offset estimators (33) and (34), respectively, versus SNR/decibel for  $n_e = 8/3$  and  $\theta_e = 0.04$ . (a) Bias and (b) MSE of  $\hat{\theta}_e$  versus  $\theta_e$ . (c) Bias and (d) MSE of  $\hat{n}_e/M$  versus  $n_e/M$ .

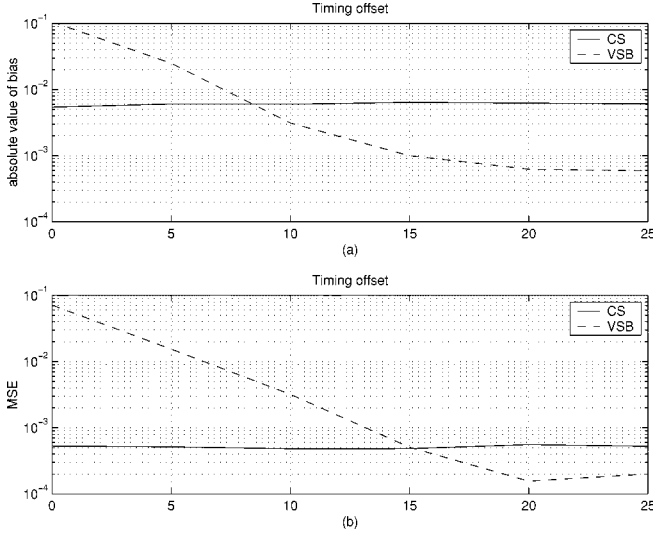


Fig. 6. Comparison between the timing estimator proposed in [13] (VSB-estimator) and the timing estimator (34) (CS-estimator) for  $\theta_e = 0$  and  $n_e = 2$ . (a) Bias and (b) MSE of  $\hat{n}_e/M$  versus  $n_e/M$  as a function of SNR.

In the high SNR regime, the VSB-estimator performs better than our estimator.

*Simulation Example 6:* In the last example, we investigate the effect of the length  $L$  of the data record used for estimating the cyclic statistics  $\hat{C}_r[k, \tau]$  on the performance of the time-frequency offset estimators (33) and (34). For  $n_e = 5$ ,  $\theta_e = 0.05$  and three different SNR values, Fig. 7(a) and (b) shows the bias and MSE, respectively, of  $\hat{\theta}_e$  versus  $\theta_e$  as a function of the length  $L$  of the data record. Fig. 7(c) and (d) shows the bias and MSE, respectively, of  $\hat{n}_e/M$  versus  $n_e/M$  as a function of  $L$ . (Note that in Fig. 7, the length of the data record has been specified in symbols. The actual length of the data record is therefore obtained by multiplying the number of symbols by 16.) The timing offset estimate has been obtained by averaging over  $\{[1, \tau] | 0 \leq \tau \leq 24\}$  and the carrier frequency offset estimator used the samples  $[k, \tau]$  with  $k = 0, 1$  and  $1 \leq \tau \leq 24$ . We

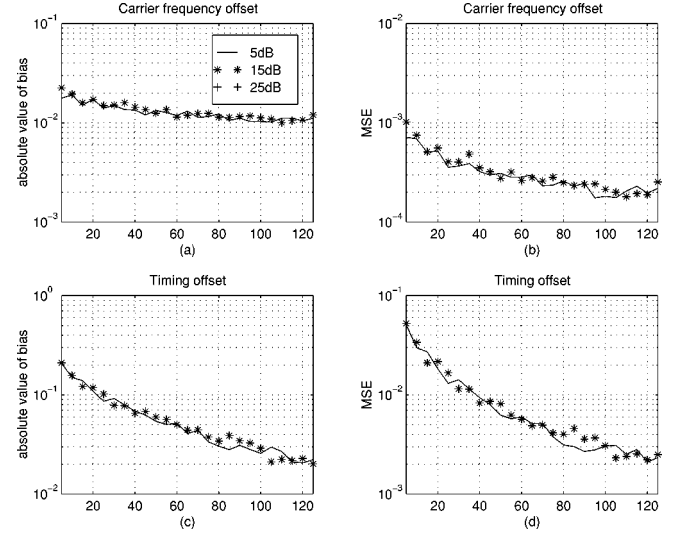


Fig. 7. Bias and MSE of carrier frequency and symbol timing offset estimators (33) and (34), respectively, versus data record length (specified in OFDM symbols) for  $\theta_e = 0.05$  and  $n_e = 5$  and three different SNR values. (a) Bias and (b) MSE of  $\hat{\theta}_e$  versus  $\theta_e$ . (c) Bias and (d) MSE of  $\hat{n}_e/M$  versus  $n_e/M$  as a function of SNR.

can see that the performance of the estimators improves with increasing data record length and that it is virtually independent of the SNR. (Note that the 25-dB curves are covered by the 15-dB curves and can therefore not be seen in the figure.)

## VI. CONCLUSIONS

We introduced a novel algorithm for the blind estimation of symbol timing errors and carrier frequency offsets in pulse shaping OFDM/QAM and OFDM/OQAM systems. Our method is based on the Gini-Giannakis estimator [1] for the single-carrier case and exploits the cyclostationarity of OFDM signals. The proposed estimators are computationally efficient (FFT-based) and allow to perform a carrier frequency acquisition over the entire bandwidth of the OFDM signal. Furthermore, the use of a special form of periodic transmitter precoding yields a symbol timing acquisition range of arbitrary length. The estimators are asymptotically unbiased and consistent. Our approach applies to noninteger timing errors as well, and we demonstrated that it needs neither pilot symbols nor a cyclic prefix. Finally, we provided simulation examples demonstrating the performance of the novel method. Specifically, we showed that besides having wider applicability, our estimators also have comparable performance to the estimators proposed in [13].

## APPENDIX

From (5), we obtain

$$c_r[n, \tau] = \mathcal{E} \left\{ e^{j(2\pi\theta_e n + \phi)} \int_0^1 X(e^{j2\pi\mu}) e^{j2\pi\mu(n-n_e)} d\mu \right. \\ \cdot e^{-j(2\pi\theta_e(n-\tau) + \phi)} \int_0^1 X^*(e^{j2\pi\nu}) \\ \cdot e^{-j2\pi\nu(n-\tau-n_e)} d\nu \left. \right\} + c_\rho[\tau]$$

which using

$$X(e^{j2\pi\theta}) = \sum_{k=0}^{N-1} w[k] G\left(e^{j2\pi(\theta - \frac{k}{N})}\right) \sum_{l=-\infty}^{\infty} c_{k,l} e^{-j2\pi l M \theta}$$

where  $G(e^{j2\pi\theta}) = \sum_{n=-\infty}^{\infty} g[n] e^{-j2\pi n \theta}$  yields

$$\begin{aligned} c_r[n, \tau] &= \sigma_c^2 e^{j2\pi\theta_e \tau} \int_0^1 \int_0^1 e^{j2\pi(n-n_e)(\mu-\nu)} e^{j2\pi\nu\tau} \\ &\cdot \sum_{k=0}^{N-1} |w[k]|^2 G\left(e^{j2\pi(\mu-(k/N))}\right) G^*\left(e^{j2\pi(\nu-(k/N))}\right) \\ &\cdot \underbrace{\sum_{l=-\infty}^{\infty} e^{j2\pi l M(\nu-\mu)}}_{(1/M) \sum_{s=0}^{M-1} \delta(\nu-\mu-(s/M))} d\mu d\nu + c_p[\tau]. \end{aligned} \quad (37)$$

Now, with  $g[n] = \int_0^1 G(e^{j2\pi\theta}) e^{j2\pi n \theta} d\theta$ , we obtain

$$\begin{aligned} c_r[n, \tau] &= \frac{\sigma_c^2}{M} e^{j2\pi\theta_e \tau} \Gamma_N[\tau] \sum_{u=-\infty}^{\infty} g[u] g[u - \tau] \\ &\cdot \sum_{s=0}^{M-1} e^{-j2\pi(s/M)(u-n+n_e)} + c_p[\tau] \end{aligned} \quad (38)$$

where  $\Gamma_N[\tau] = \sum_{k=0}^{N-1} |w[k]|^2 e^{j2\pi(k/N)k\tau}$ . For  $n_e \in \mathbb{Z}$ , using  $\sum_{s=0}^{M-1} e^{-j2\pi(s/M)(u-n+n_e)} = M \sum_{l=-\infty}^{\infty} \delta[u-n+n_e+lM]$ , (38) can be simplified to yield

$$\begin{aligned} c_r[n, \tau] &= \sigma_c^2 e^{j2\pi\theta_e \tau} \Gamma_N[\tau] \sum_{l=-\infty}^{\infty} g[n - n_e - lM] \\ &\cdot g[n - n_e - lM - \tau] + c_p[\tau]. \end{aligned}$$

For  $n_e \in \mathbb{R}$ , the Fourier series coefficients  $C_r[k, \tau] = (1/M) \sum_{n=0}^{M-1} c_r[n, \tau] e^{-j(2\pi/M)kn}$  of  $c_r[n, \tau]$  with respect to  $n$  are given by

$$\begin{aligned} C_r[k, \tau] &= \frac{\sigma_c^2}{M^2} e^{j2\pi\theta_e \tau} \Gamma_N[\tau] \sum_{u=-\infty}^{\infty} g[u] g[u - \tau] \\ &\cdot \sum_{s=0}^{M-1} e^{-j2\pi(s/M)(u+n_e)} \\ &\cdot \underbrace{\sum_{n=0}^{M-1} e^{-j2\pi(n/M)(k-s)}}_{M\delta[k-s]} + c_p[\tau] \delta[k] \\ &= \frac{\sigma_c^2}{M} e^{j2\pi\theta_e \tau} \Gamma_N[\tau] \sum_{u=-\infty}^{\infty} g[u] g[u - \tau] \\ &\cdot e^{-j2\pi(k/M)(u+n_e)} + c_p[\tau] \delta[k] \\ &= \frac{\sigma_c^2}{M} e^{j2\pi\theta_e \tau} e^{-j(2\pi/M)kn_e} \Gamma_N[\tau] A^{(g,g)}\left[\tau, \frac{k}{M}\right] \\ &+ c_p[\tau] \delta[k]. \end{aligned} \quad (39)$$

## ACKNOWLEDGMENT

The author would like to thank Prof. W. Mecklenbräuker and Prof. F. Hlawatsch for useful discussions and the anonymous reviewers for their comments.

## REFERENCES

- [1] F. Gini and G. B. Giannakis, "Frequency offset and symbol timing recovery in flat-fading channels: A cyclostationary approach," *IEEE Trans. Commun.*, vol. 46, pp. 400–411, Mar. 1998.
- [2] A. Peled and A. Ruiz, "Frequency domain data transmission using reduced computational complexity algorithms," in *Proc. IEEE ICASSP'80*, Denver, CO, 1980, pp. 964–967.
- [3] L. J. Cimini, "Analysis and simulation of a digital mobile channel using orthogonal frequency division multiplexing," *IEEE Trans. Commun.*, vol. 33, pp. 665–675, July 1985.
- [4] M. Sandell, "Design and analysis of estimators for multicarrier modulation and ultrasonic imaging," Ph.D. dissertation, Lulea Univ. Technol., Lulea, Sweden, 1996.
- [5] R. Haas, "Application des transmissions à porteuses multiples aux communications radio mobiles," Ph.D. dissertation, Ecole Nationale Supérieure des Télécommunications, Paris, France, Jan. 1996.
- [6] B. LeFloch, M. Alard, and C. Berrou, "Coded orthogonal frequency division multiplex," *Proc. IEEE*, vol. 83, pp. 982–996, June 1995.
- [7] T. Pollet and M. Moeneclaey, "The effect of carrier frequency offset on the performance of band limited single carrier and OFDM signals," in *Proc. IEEE GLOBECOM'96*, vol. 1, London, U.K., 1996, pp. 719–723.
- [8] W. D. Warner and C. Leung, "OFDM/FM frame synchronization for mobile radio data communication," *IEEE Trans. Veh. Technol.*, vol. 42, no. 3, pp. 302–313, 1993.
- [9] P. H. Moose, "A technique for orthogonal frequency division multiplexing frequency offset correction," *IEEE Trans. Commun.*, vol. 42, pp. 2908–2914, Oct. 1994.
- [10] M. Luise and R. Reggiannini, "Carrier frequency acquisition and tracking for OFDM systems," *IEEE Trans. Commun.*, vol. 44, pp. 1590–1598, Nov. 1996.
- [11] T. M. Schmidl and D. C. Cox, "Robust frequency and timing synchronization for OFDM," *IEEE Trans. Commun.*, vol. 45, pp. 1613–1621, Dec. 1997.
- [12] F. Daffara and O. Adami, "A new frequency detector for orthogonal multicarrier transmission techniques," in *Proc. IEEE VTC'95*, vol. 2, Chicago, IL, July 1995, pp. 804–809.
- [13] J.-J. van de Beek, M. Sandell, and P.-O. Börjesson, "ML estimation of timing and frequency offset in OFDM systems," *IEEE Trans. Signal Processing*, vol. 45, pp. 1800–1805, July 1997.
- [14] W. A. Gardner, Ed., *Cyclostationarity in Communications and Signal Processing*. Piscataway, NJ: IEEE Press, 1995.
- [15] W. Kozek and A. F. Molisch, "Robust and efficient multicarrier communication by nonorthogonal Weyl–Heisenberg systems," *IEEE J. Select. Areas Commun.*, vol. 16, pp. 1579–1589, Oct. 1998.
- [16] H. Bölcskei, P. Duhamel, and R. Hleiss, "Design of pulse shaping OFDM/OQAM systems for high data-rate transmission over wireless channels," in *Proc. IEEE Int. Conf. Communications (ICC)*, Vancouver, BC, Canada, June 1999, pp. 559–564.
- [17] B. Hirosaki, "An orthogonally multiplexed QAM system using the discrete Fourier transform," *IEEE Trans. Commun.*, vol. COM-29, pp. 982–989, July 1981.
- [18] R. Haas and J. C. Belfiore, "A time-frequency well-localized pulse for multiple carrier transmission," *Wireless Pers. Commun.*, vol. 5, pp. 1–18, 1997.
- [19] R. Tolimieri and M. An, *Time-Frequency Representations*. Boston, MA: Birkhäuser, 1998.
- [20] M. de Courville, "Utilization de bases orthogonales pour l'algorithme adaptative et l'egalization des systèmes multiporteuses," Ph.D. dissertation, Ecole Nationale Supérieure des Télécommunications, Paris, France, Oct. 1996.
- [21] M. Vetterli, "A theory of multirate filter banks," *IEEE Trans. Acoust., Speech, Signal Processing*, vol. ASSP-35, pp. 356–372, Mar. 1987.
- [22] L. L. Scharf, *Statistical Signal Processing*. Reading, MA: Addison-Wesley, 1991.
- [23] A. V. Dandawate and G. B. Giannakis, "Asymptotic theory of mixed time averages and  $k$ th-order cyclic-moment and cumulant statistics," *IEEE Trans. Inform. Theory*, vol. 41, pp. 216–232, 1995.
- [24] A. V. Dandawate and G. B. Giannakis, "Nonparametric polyspectral estimators for  $k$ th-order (almost) cyclostationary processes," *IEEE Trans. Inform. Theory*, vol. 40, pp. 67–84, 1994.



**Helmut Bölcskei** (S'94–M'98) was born in Austria on May 29, 1970. He received the Dipl.-Ing. and Dr. Techn. degrees from Vienna University of Technology, Vienna, Austria, in 1994 and 1997, respectively.

From December 1994 to February 2001, he was with the Department of Communications and Radio-Frequency Engineering, Vienna University of Technology, Vienna, Austria. Since March 2001, he has been an Assistant Professor of Electrical Engineering at the University of Illinois at Urbana-Champaign.

From February to May 1996, he was a Visiting Researcher with the Applied Mathematics Group at Philips Research Laboratories, Eindhoven, The Netherlands. From February to March 1998, he visited ENST Paris. From February 1999 to February 2001, he did postdoctoral research in the Smart Antennas Research Group in the Information Systems Laboratory, Department of Electrical Engineering, Stanford University, Stanford, CA. His research interests include wireless communications and communication theory with special emphasis on multi-antenna (MIMO) systems, OFDM, high-speed wireless networks, and parameter estimation problems in the context of wireless communications.

Dr. Bölcskei is presently serving as an Associate Editor for the IEEE TRANSACTIONS ON SIGNAL PROCESSING.